

國立交通大學

應用數學系

碩士論文

出現在生物學中分段光滑映射之混沌與分裂

Chaos and Bifurcation of Piecewise Smooth Maps

Arising in Ecology



研究生：鄧仁益

指導教授：莊重 教授

中華民國 一〇二 年 五 月

出現在生物學中分段光滑映射之混沌與分裂

Chaos and Bifurcation of Piecewise Smooth Maps

Arising in Ecology

研究生：鄧仁益

Student：Ren-Yi Deng

指導教授：莊重 教授

Advisor：Jonq Juang



Submitted to Department of Applied Mathematics
College of Science

National Chiao Tung University

In Partial Fulfillment of the Requirements
for the Degree of Master

in

Applied Mathematics

June 2013

Hsinchu, Taiwan, Republic of China

中華民國 一〇二年 五月

出現在生物學中分段光滑映射之混沌與分裂

研究生：鄧仁益

指導教授：莊重 教授

國立交通大學

應用數學系

摘要

本論文包含兩個部分。在第一部分中，我們考慮一個廣義生態資源預算模型，有一個參數 d ，是由一匝 [1]、沙他和岩佐 [2] 的資源模型預算來的。這裡的 d 是耗盡係數。張書銘 [3] 藉由拓撲商是正的當 $d > 1.00026$ 來證明該模型有德瓦尼的混亂在不變的集合上。我們改進了他們的結果藉由此模型有正的拓撲商當 $d > 1$ 。在第二部分，我們研究了路徑到混亂的另一個分段光滑映射，此映射是由一匝、沙他和岩佐 [1-2] 同步的森林模型來的。這樣的映射包含兩個參數 d 和 β 。這裡的 β 是指樹跟樹之間的交配花粉可用性的耦合強度。這是透過數值展現，這種分段光滑映射路徑到混亂是通過有限的兩倍週期分岔。我們藉由提供了幾個應用上的例子去進一步說明這種路徑到混亂是通用的對於分段光滑映射。

中華民國 一〇二 年 五 月

Chaos and Bifurcation of Piecewise Smooth Maps Arising in Ecology

Student : Ren-Yi Deng

Advisor : Jonq Juang

Department of Applied Mathematics
National Chiao Tung University

Abstract

This thesis contains two parts. In the first part, we consider a generalized resource budget model of ecology with a parameter d , which was modified from Isagi [1] resource budget model by Staka and Iwasa [2]. Here d is the depletion coefficient. Shu-Ming Chang [3] thought that the model was shown that the model has Devaney's chaos on an invariant set by proving its topological entropy is positive for $d > 1.00026$. We improve their result by proving that the map had positive topological entropy for $d > 1$. In this second part, we study the route to chaos for another piecewise smooth map, which governs the synchronized dynamics of the forest model of Isagi-Staka-Iwasa [1-2]. Such map contains two parameters d and β . Here β denotes the coupling strength among the trees in their outcross pollen availability. It is numerically demonstrate that the route to chaos of such piecewise smooth map is through finite period doubling bifurcation. We further illustrate such route to chaos is generic for piecewise smooth maps by providing several examples arising in application.

May 2013

誌謝

我的碩士學位能夠順利地獲得最需要感謝的人是我的指導教授莊重教授，念碩士班的過程中他給予了我相當多的書本知識以及對數學的見解；讓我了解到念數學不僅只是把定義、定理看懂而已，最主要的就是培養對它的感覺，要能夠用自己的話說出核心概念；除此之外，面對問題時可以先想想看如何用最少的力氣去解決它，也就是說對問題要能夠分析清楚，才能順利地突破盲點；這些對我來說不是很難做到，但從莊重教授一次又一次的示範當中，慢慢能夠體會對數學的感覺。

家人是我努力的原動力。因為媽媽、阿姨、舅舅、舅媽他們對我不求回報的付出，讓我不用去煩惱其它事情，也不需要特地的聊天或出去玩來聯絡親情，一切都以不影響我的讀書、課業為主，我才能安心的在課業上奮鬥，所以對家人我只有滿滿的感謝。

念書、做研究是一條漫長的道路，要能夠接受考驗，可能一次就成功，但也可能做了好久、換了好多方法還是失敗，所以心情的調適和轉換就變得很重要了。因此，要謝謝我非常貼心的女朋友，在我煩悶時聽我訴苦，使我的情緒找到了出口；放假日時一起去散心、給我鼓勵，讓我更有元氣、精神去做研究，提高我的讀書效率。謝謝她的體貼、包容，讓我更專注在課業上。

運動也是提升讀書效率的好方法之一，因為運動完後腦中會分泌一種物質叫腦內啡，使人心情感到愉悅，就可以忘記運動前讀書時所遇到的挫折。所以，很慶幸在研究所時遇到一群愛好運動的同學們，平常大家就會一起約去打球，在球場上奮力地揮灑自己的汗水；運動完後，再一起吃飯、聊天，好不快樂，之後又可以繼續埋首苦讀，一起討論功課。所以很感謝這些好同學們，讓我在做研究的路上不孤單，大家一起互相扶持的感覺真的很棒！

國立交通大學

研究所碩士班

論文口試委員會審定書

本校應用數學系 _____ 鄧仁益 _____ 君
所提論文

Chaos and Bifurcation of Piecewise Smooth
Maps Arising in Ecology

合於碩士資格水準，業經本委員會評審認可。

口試委員： 張學勤 莊重

蔡龍

指導教授： 莊重

系主任： 陳昭明

中華民國 102 年 05 月 15 日

Contents

1	Introduction	1
1.1	Isagi's energy budget	3
1.2	Satake and Iwasa's generalized energy budget	4
2	Preliminaries	5
2.1	Devaney's chaos	5
2.2	Topological entropy	6
3	Mathematical analysis	7
4	Finite period doubling route to chaos	10
4.1	Numerical Simulations	13
4.2	Applications	18
5	Conclusion	23

1 Introduction

In this thesis, we shall investigate chaos and bifurcation of a certain piecewise smooth maps arising in ecology. Several explanations of the masting phenomenon in a mature forest have been proposed [4-25]. They involve environmental fluctuations, weather conditions, swamping predators, the weight of young deer, bird populations, the reproductive success of bears, increased efficiency of wind pollination, attraction to seed distributions, cue masting, and the dispersing of animals. However, most of these hypotheses explain neither the mechanism of masting nor the mechanism by which the timing of reproduction

varies among individuals [2]. In [1], Isagi considered the energy budget of an individual tree describing how its energy is accumulated and used. It was later generalized by Stake and Iwasa [2]. Such map is a nonsmooth map containing a parameter d . Such parameter d denotes the degree of energy depletion of a tree after its reproductive year. In [3], the model was shown to have Devaney's chaos on an invariant set by proving its topological entropy is positive for $d > 1.00026$. We improve their result by proving that the map had positive topological entropy for $d > 1$.

In [2], a couple map lattices was proposed to explain how a mature forest mast and synchronize by considering outcross pollen availability among trees. Various synchronized reproductions such an annual reproduction, periodic and chaotic reproductions were observed. To understand such synchronized phenomenon, we are led to study another nonsmooth map that governs the dynamics on the synchronized manifold of the map lattices. Such map contains two parameters d and β . Here β denotes the coupling strength among the trees in their outcross pollen availability. It is numerically demonstrate that the route to chaos of such piecewise smooth map is through finite period doubling bifurcation.

Nature is full of piecewise smooth nonlinearities. That is, their evolution is characterized by periods of smooth notion interrupted by instantaneous crossings of boundaries separating regions of phase space where different smooth models apply. Such problems arise naturally from many kinds of engineering systems. Examples include the stick-slip oscillations of a violin string or grating brakes [26], the cam-follower system and the impact oscillator in mechanical applications [27], many problems in electronics [28] and neuron-firing models [29]. Much attention have been drawn to the study of their surprisingly rich (chaotic) dynamics. Less mentioned is their routes to chaos, which are well studied for smooth systems. In this paper we identify a route to chaos, which is termed the finite period-doubling. The mechanism for the occurrence of such routes is also discussed. Several examples arising in the real applications are provided

for illustration.

Transition to chaos, i.e., how a system becomes chaotic as a parameter of the system changes, has been a fundamental and central problem [30] in the study of nonlinear dynamical systems. In particular, the transition route to chaos in smooth dynamical systems have been well understood. This transition often occurs via the following four known routes: (i) the period-doubling cascade route [31], (ii) the intermittency transition route [32], (iii) the crisis route [33], and (iv) the route to chaos in quasi-periodically driven systems [34-35]. On the other hand, the case that how a nonsmooth dynamical system gives rise to chaos remains a less-studied area. By nonsmoothness, we allow a map to be continuous but not differentiable at some finite points. Such systems occur naturally in the description of physical nonsmooth processes such as impact, switching, sliding and other discrete state transitions. Literature [36-42] that draws attention to piecewise-smooth systems have been focus on their qualitative and quantitative theory. The purpose of this paper is to investigate their route to chaos. We report that a *finite period-doubling* route to chaos for a class of nonsmooth dynamical systems. Among several examples presented for illustration arise three models in real applications: a map model in ecology system [1-2] and two nonsmooth continuous-time flows: the impact oscillator (see e.g., [27,43]) and the work cited therein) and the friction oscillator and DC-DC converter (see e.g., [44]).

1.1 Isagi's energy budget

Isagi [1] considered the energy budget of an individual tree. From photosynthesis, mature tree gains net production P_s per year, which is accumulated in the trunk or branches. When the energy reserve exceeds a critical level for reproduction, the tree sets flowers and produces seeds and fruits. Let $S(t)$ be the amount of energy reserve at the beginning of year t . If the sum $S(t) + P_s$ is below a critical level L_T , the tree does not reproduce and saves all the energy reserve for the following year. However, if the sum exceeds L_T , the tree

uses energy for flowering. Isagi et al [1]. assumed that the energy expenditure for flowering is exactly the same as the excess, $S(t) + P_s - L_T$.

1.2 Satake and Iwasa's generalized energy budget

Satake and Iwasa's [2] generalize Isagi energy budget—the amount of energy expenditure for flowering is proportional to the excess, $a(S(t) + P_s - L_T)$, in which a is a positive constant. Flowering plants may be pollinated and set seeds and fruits. It is assumed that the cost for fruits is proportional to the cost of flowers, and is expressed as $R_c a(S(t) + P_s - L_T)$, in which R_c is the ratio of fruiting cost to flowering cost. After the reproductive stage, the energy reserves of the tree falls to $S(t) + P_s - a(R_c + 1)(S(t) + P_s - L_T)$. Hence, we have

$$S(t+1) = \begin{cases} S(t) + P_s, & S(t) + P_s \leq L_T, \\ S(t) + P_s - a(R_c + 1)(S(t) + P_s - L_T), & S(t) + P_s > L_T. \end{cases} \quad (1)$$

We introduce a non-dimensionalized variable $Y(t) = \frac{(S(t) + P_s - L_T)}{P_s}$. Then equation(1) is written as

$$Y(t+1) = \begin{cases} Y(t) + 1, & Y(t) \leq 0, \\ -dY(t) + 1, & Y(t) > 0, \end{cases} \quad (2)$$

in which $d = a(R_c + 1) - 1$. The parameter d indicates the degree of resource depletion after a reproductive year divided by the excess amount of energy reserve before the year. We call d the depletion coefficient, and assume $d > 0$. From equation (2) , $Y(t) \leq 0$ holds. We also note that the quantity $Y(t)$ is positive if and only if the tree invests some reproductive activity in year t .

After this rescaling, the dynamics of equation (2) include only a single parameter d . It is clear that $Y(t+1)$ goes to infinity eventually at $d < 0$. On the hand, $Y(t+1)$ belongs in $[-d + 1, 1]$ as t large enough at $d \geq 0$. Satake and Iwasa (2) illustrated trajectories for the three different of d . When $d \in [0, 1)$,

$Y(t+1)$ quickly converges to the stable equilibrium $\frac{1}{d+1}$. There are a number of two-point cycles corresponding to the different initial conditions when d exactly d is equal to 1. When $d > 1$, $Y(t+1)$ keeps fluctuating with a chaotic time series.

Through this thesis, the n -fold composition of f with itself recurs repeatedly in the sequel, f^n , and it is defined as $f^n = f \circ \dots \circ f(x)$, where n is the number of iterations. The generalized resource budget model (2) can be represented as a map f ,

$$f(x) = \begin{cases} x + 1, & x \leq 0, \\ -dx + 1, & x > 0. \end{cases} \quad (3)$$

2 Preliminaries

2.1 Devaney's chaos

The chaos of map has been defined in several ways. Although the comment "so many authors, so many definitions," is true, a basic component of all definitions is the unpredictability of the behavior of the trajectory which is determined with some certain error. (The associated phenomenon is usually described in terms of sensitive dependence on initial conditions). The definition of the chaos of Devaney [45] is considered herein because it is fundamental and widely accepted.

Definition 2.1. *Let X be a metric space. A continuous map $f : X \rightarrow X$ is said to be chaotic on X if*

(Sensitive): *f has sensitive dependence on initial condition, meaning that there $\delta > 0$ such that, for any $x \in X$ and any neighborhood N_x of x , there exists $y \in N_x$ and $n \in \mathbb{N}$ such that $|f^n(x) - f^n(y)| > \delta$.*

(Density): *periodic points are dense in X ;*

(Transitivity): *f is topologically transitive. That is, for any pair of nonempty open sets $U, V \subset X$, there exists $k > 0$ such that $f^k(U) \cap V \neq \emptyset$.*

2.2 Topological entropy

Definition 2.2. Let $f : X \rightarrow X$ be a continuous map on the space X which is compact with metric d . A set $S \subset X$ is called (n, ϵ) -separated for f for n positive integer and $\epsilon > 0$ provided that for every pair $\mathbf{x}, \mathbf{y} \in S$, $\mathbf{x} \neq \mathbf{y}$, there is at least one k with $0 \leq k < n$ such that $d(f^k(x), f^k(y)) > \epsilon$. The number of different orbits of length n (as measured by ϵ) is defined by

$$r(n, \epsilon, f) = \max\{\#(S) : S \subset X \text{ is } (n, \epsilon) \text{- separated set for } f\},$$

where $\#(S)$ is the cardinality of elements in S . Let

$$h_{top}(\epsilon, f) = \limsup_{n \rightarrow \infty} \frac{\log(r(n, \epsilon, f))}{n}$$

and define the **topological entropy** (46) of f as

$$h_{top}(f) = \lim_{\epsilon \rightarrow 0, \epsilon > 0} h_{top}(\epsilon, f).$$

Consider the continuous map on the compact interval, the relationship between positive topological entropy ($h_{top}(f) > 0$) and Devaney's chaos is equivalent.

Theorem 2.1. Let f be a continuous map of a compact interval I to itself, f has positive topological entropy if and only if f is chaotic in the sense of Devaney on a closed invariant set in I [47-50].

The basic result following that is used to help calculate the entropy, and relates the entropy of a map f to a n -fold composition of f , f^n .

Theorem 2.2. Assume $f : X \rightarrow X$ is uniformly continuous or X is compact, and n is an integer with $n \geq 1$. Then $h_{top}(f^n) = n \cdot h_{top}(f)$ [46].

There is another way to calculate topological entropy was defined by Welington and Sebastian [51].

Definition 2.3. Let $f : I \rightarrow I$ be a continuous piecewise monotone map. The lap number of f , which we defined $\ell(f)$ is the number of, maximal intervals on which f is monotone. In other words, $\ell(f) - 1$ is the number of turning points of f [51].

Theorem 2.3. (Misiurewicz and Szlenk). Let $f : I \rightarrow I$ be a continuous, piecewise monotone map. Then the topological entropy of f is equal to the logarithm of the number $s(f) = \lim_{n \rightarrow \infty} (\ell(f^n))^{\frac{1}{n}}$ [51].

3 Mathematical analysis

In this section, we will prove that the generalized resource budget model is chaotic in the sense of Devaney on a closed invariant set in $[1 - d, 1]$ when the depletion coefficient d is greater than 1 by using the preliminaries, the topological entropy theory.

Theorem 3.1. f is finitely renormalizable when the depletion coefficient d is greater than 1.

Proof. We have the recursion of slope of equation f algebraically.

$$x_{n+1} = \begin{cases} x_n x_n, & n \text{ is odd,} \\ x_n y_n, & n \text{ is even,} \end{cases}$$

$$y_{n+1} = \begin{cases} x_n y_n, & n \text{ is odd,} \\ y_n y_n, & n \text{ is even,} \end{cases}$$

where $x_1 = -d$, $y_1 = (-d)^2$, x_n and y_n represent the slopes of left part and right part of function f^{2^n} in the box, respectively. Hence, by the recursion, we

can conclude that

$$a_n = \sum_{k=0}^{\frac{n-1}{2}} 2^{2k}, b_n = a_n + 1, \text{ where } n \text{ is odd.}$$

$$a'_n = \sum_{k=0}^{\frac{n}{2}-1} 2^{2k+1}, b'_n = a'_n + 1, \text{ where } n \text{ is even,}$$

where a_n, b_n are the power of slopes of left part and right part of f^{2^n} in the box if n is odd, respectively. It's the same meaning to a'_n, b'_n when n is even. Assume the hump of f^{2^n} stay in the box then we have

$$f^{(2^{n+1})}(0) = f^{(2^n)}(0)[1 + (-d)^{a_n}], \text{ where } n \text{ is odd.}$$

$$f^{(2^{n+1})}(0) = f^{(2^n)}(0)[1 + (-d)^{b'_n}], \text{ where } n \text{ is even.}$$

Now, we want to express fixed point and its preimage of f^{2^n} in the box if n is odd or n is even. First, n is odd, solve the fixed point for the following equation:

$$f_{left}^{(2^n)}(x) = (-d)^{a_n}x + f^{(2^n)}(0),$$

where $f_{left}^{(2^n)}(x)$ means the equation of f^{2^n} 's left part in the box. Thus $x^* = \frac{f^{(2^n)}(0)}{1 - (-d)^{a_n}}$ is the fixed point of it. Moreover, solve the solution x_{-1}^* of equation:

$$(-d)^{a_n+1}x + f^{(2^n)}(0) = x^*,$$

then $x_{-1}^* = \frac{f^{(2^n)}(0)}{(-d)^{a_n+1}} [\frac{1}{1 - (-d)^{a_n}} - 1]$. Thus, if $n > \frac{\log(\frac{\log(d+1)}{\log d})}{\log(2)}$ then $f^{(2^{n+1})}(0) > x_{-1}^*$. That is, $f^{2^{n+1}}$ protrudes through the top of the box. Second, for n is even.

Continuing the calculation process is like above described. Therefore, $y^* = \frac{f^{(2^n)}(0)}{1 - (-d)^{b'_n}}$ is the fixed point of f^{2^n} in the box and $y_{-1}^* = \frac{f^{(2^n)}(0)}{(-d)^{b'_n}} [\frac{1}{1 - (-d)^{b'_n}} - 1]$.

Hence, if $n > \frac{\log(\frac{\log(d(d+1))}{\log d})}{\log(2)}$ then $f^{(2^{n+1})}(0) < y_{-1}^*$. That is, $f^{2^{n+1}}$ protrudes through the bottom of the box. Furthermore, we want to find the exactly n_0 such that $f^{(2^{n_0+1})}(0) > x_{-1}^*$ or $f^{(2^{n_0+1})}(0) < y_{-1}^*$. Define $y = \frac{\log(\frac{\log(d(d+1))}{\log d})}{\log(2)}$ and $x = \frac{\log(\frac{\log(d+1)}{\log d})}{\log(2)}$. Thus, for $d > 1$, we have $y, x > 0$ and $0 < y - x =$

$\frac{\log(\frac{\log(d)}{\log(d+1)}+1)}{\log(2)} < 1$. There are three possibilities for choosing n_0 which is related to y and x .

1. $n_0 - 1 < x < y < n_0$, then choose x such that $f^{(2^{n_0+1})}(0) > x_{-1}^*$, where n_0 is odd.
2. $n_0 - 1 < x < y < n_0$, then choose y such that $f^{(2^{n_0+1})}(0) < y_{-1}^*$, where n_0 is even.
3. $x < n_0 - 1 < y < n_0$, then choose x such that $f^{(2^{n_0+1})}(0) > x_{-1}^*$, where n_0 is odd.

Hence, f is finitely renormalizable when the depletion coefficient d is greater than 1. □

Theorem 3.2. $h_{top}(f)$ is no less than $\frac{\ln 2}{2^{n_0+1}}$ when the depletion coefficient d is greater than 1.

Proof. We want to demonstrate that $f^{2^{n_0+1+n}}$ has 2^{n-1} peaks on $[x^*, x_{-1}^*]$ for n_0 in theorem 3.1. Define $f^{2^{n_0+1}} = h$ and the proof is by mathematical induction on n . The result is immediate if $n = 1$. Suppose that the result is true for $n = k$. That is, h^k has 2^{k-1} peaks. Consider $n = k + 1$, we denote respectively that x_1, \dots, x_{k-1} is the x -coordinate of the $k - 1$ peaks, and z_{i_1}, z_{i_2} are the height of the lowest of the peaks with $h(z_{i_1}) = h(z_{i_2}) = x^*$, for $i = 1, \dots, k - 1$. Moreover, we know that there are two points denoted y_{i_1}, y_{i_2} of each peak with $y_{i_1} < y_{i_2}$ and $h(y_{i_1}) = h(y_{i_2}) = x_{-1}^*$, for $i = 1, \dots, k - 1$. Besides, h^k is continuous and monotone on each interval $[z_{i_1}, z_{i_2}]$, for $i = 1, \dots, k - 1$. Thus, we can find two points $x_{i_1}^{-1} \in (z_{i_1}, x_i)$ and $x_{i_2}^{-1} \in (x_i, z_{i_2})$ such that $h(x_{i_1}^{-1}) = h(x_{i_2}^{-1}) = x_i$, for $i = 1, \dots, k - 1$. Furthermore, we also can find $y_{i_{11}}^{-1}, y_{i_{12}}^{-1} \in (z_{i_1}, x_i)$ such that $h(y_{i_{11}}^{-1}) = h(y_{i_{12}}^{-1}) = y_{i_1}$ and $y_{i_{21}}^{-1}, y_{i_{22}}^{-1} \in (y_{i_1}, z_{i_2})$ such that $h(y_{i_{21}}^{-1}) = h(y_{i_{22}}^{-1}) = y_{i_2}$, for $i = 1, \dots, k - 1$. Therefore, it becomes two peaks of h^{k+1} on $[z_{i_1}, z_{i_2}]$ by Intermediate Value Theorem, for $i = 1, \dots, k - 1$. Hence, there are $2 \times 2^{k-1}$ peaks for function h^{k+1} on $[x^*, x_{-1}^*]$ and so h^n has 2^{n-1} peaks. On the other hand, because we get $\ell(f^{2^{n_0+1}}) = \ell(h^n) = 2 \times 2^{n-1} = 2^n$,

$h_{top}(f^{2^{n_0+1}}|_{[x^*, x_{-1}]}) = \ln 2$ by theorem2.3. Then, $h_{top}(f^{2^{n_0+1}})$ is no less than $\ln 2$ on the compact set $[1 - d, 1]$. Finally, the result shows that $h_{top}(f)$ is no less than $\frac{\ln 2}{2^{n_0+1}}$ by theorem2.2. \square

Theorem 3.3. *The generalized resource budget model is chaotic in the sense of Devaney on a closed invariant set in $[1 - d, 1]$ when the depletion coefficient d is greater than 1.*

Proof. We have $h_{top}(f) > 0$ for $d > 1$ according to the theorem3.2. Therefore, f is chaotic in the sense of Devaney on a closed invariant set in $[1 - d, 1]$ by theorem2.1. Hence, the result shows that the map f can possess Devaney's chaos when the depletion coefficient d is greater than 1. \square

4 Finite period doubling route to chaos

Usually the term "route to chaos" refers to formation of chaotic attractors. In this section, we consider route from a parameter having no chaos to one with chaotic sets, where the sets are not necessarily attractors. To be more precise, we require only one aspect of chaos: we say that a map has a chaos at a particular μ if there exist infinitely many periodic orbits; otherwise, it is said that the map has no chaos at the particular μ . For example either one of the following conditions is sufficient for a continuous map to have chaos. (i) The positivity of the topological entropy (see e.g. [52]). (ii) The existence of a horseshoe [53]. (iii) The existence of a nondegenerate homoclinic orbit [54]. (iv) The existence of a periodic point with its period being not the power of two. (v) The map is finitely renormalizable [52]. The concepts of a horseshoe and being finitely renormalizable are to be used through out this section. The definition of the latter, which is more complicated, is to be given at the appropriate place. If $I \subset \mathbb{R}$ is a closed interval, $f : I \rightarrow \mathbb{R}$ continuous, and $a < c < b \in I$, then we say that $[a, b]$ is a horseshoe for f if $[a, b] \subset f([a, c]) \cap f([c, b])$. The presence of a horseshoe clearly produces a full two-shift as a factor of the restriction of

f to an invariant set. Consequently, f has periodic points of all period and its topological entropy is no less than $\ln 2$.

For smooth dynamical systems that depend on a parameter, one of the basic route to chaos is the period-doubling cascade. For instance, it is well-known that for the quadratic family $f_\mu(x) = \mu x(1-x)$, the route to chaos is through period-doubling. A geometric and intuitive answer to the process can be provided as follows.

For $0 \leq \mu \leq 3$, f_μ has a globally attracting fixed point. Before f_μ can possibly have infinitely many periodic points with distinct periods, it must have periodic points with all periods of the form 2^j according to Sarkovskii's Theorem (see e.g., (54)). That leads to the consideration of the graph of f_μ^2 which resembles the graph of the original quadratic map (for a different μ -value). Using graphical analysis of f_μ , we may also sketch the graphs of f_μ^2 for various μ -values. These are depicted in Fig 1. Note that in Fig 1-c, we say that $[\hat{p}_{\mu,0}, p_{\mu,0}]$ is a horseshoe for f^2 . Inside the box, f_μ^2 has one fixed point $p_{\mu,0}$ at an endpoint of the interval $[\hat{p}_{\mu,0}, p_{\mu,0}]$ and a unique critical point with this interval. Note that, as long as $f'_\mu(p_{\mu,0}) < 0$ (resp., > 0), there exists a "partner" $\hat{p}_{\mu,0}$ for $p_{\mu,0}$ in the sense that $f_\mu(\hat{p}_{\mu,0}) = p_{\mu,0}$ and $\hat{p}_{\mu,0} < p_{\mu,0}$ (resp., $\hat{p}_{\mu,0} > p_{\mu,0}$). As μ increases, we first expect a new fixed point $p_{\mu,1}$ in $[\hat{p}_{\mu,0}, p_{\mu,0}]$ for f_μ^2 (i.e., a period 2 point for f_μ) to be born. Eventually, this "fixed point" will itself period-double, just as $p_{\mu,0}$ did for f_μ , producing a period 4 point. Continuing the procedure, we may find a small box in which the graphs of f_μ^4 , f_μ^8 , etc., resemble the original quadratic function. Such ideas can be made precise, by using the so called renormalization techniques. Thus we are led to expect that f_μ undergoes a series of period-doublings as μ increases. On the other hand, if one views this process algebraically, then at the bifurcation value $\mu_1 = 3$ for the family f_μ , the fixed point changes from attracting for $1 < \mu < \mu_1$ to repelling for $\mu > \mu_1$. For μ slightly larger than μ_1 , the 2-period orbit is born and is attracting. As μ moves past μ_2 , where the period four orbit is created and is attracting. Again, the original 2-periodic orbit changes from attracting to repelling. Such period

four orbit becomes repelling for $\mu > \mu_3$ and a new attracting period eight orbit is born. This process repeats itself; at $\mu > \mu_n^+$, the period 2^n orbit is added. This orbit is attracting for $\mu_n < \mu < \mu_{n+1}$ and becomes repelling for $\mu > \mu_{n+1}$.

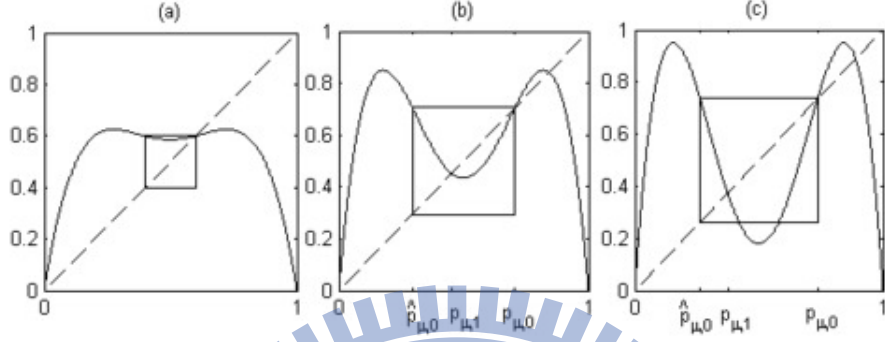


Figure 1: The graphs of $f_\mu^2(x)$ for $\mu = 2.5$, $\mu = 3.4$ and $\mu = 3.8$, respectively.

Now, combining the geometric and algebraic view together, we have that for $\mu_n < \mu < \mu_{n+1}$, the corresponding box containing the graph of $f_\mu^{2^n}$, i.e., the graph of $f_\mu^{2^n}$ on $[p_{\mu,n-1}, \hat{p}_{\mu,n-1}]$ if n is even or on $[\hat{p}_{\mu,n-1}, p_{\mu,n-1}]$ if n is odd, is similar to that of in Fig 1-(b). Here $p_{\mu,n}$ is the 2^n periodic point of f . However, for the same range of μ , the associated box containing the graph of $f_\mu^{2^{n+1}}$ is similar to that of in Fig 1-(a). As a result, the parameters in this range yield no new fixed point, and hence, no chaos. It should be mentioned that for $\mu_{n+1} < \mu < \mu_{n+2}$, the graph of $f_\mu^{2^{n+1}}$ in the corresponding box is similar to that of in Fig 1-(b). Such sequence $\{\mu_n\}$ produces a universal constant as the rate of convergence. For $\mu_\infty := \lim_{n \rightarrow \infty} \mu_n$, f_{μ_∞} is called infinitely renormalizable. Geometrically speaking, this means that for any n , the graph of $f_{\mu_\infty}^{2^n}$ on the corresponding box has the following two properties:

- (i) there exists a fixed point in $(\hat{p}_{\mu,n-1}, p_{\mu,n-1})$ or $(p_{\mu,n-1}, \hat{p}_{\mu,n-1})$ for $f_{\mu_\infty}^{2^n}$;
- (ii) the "hump" will not extend out the box.

Pictorially, this means that for any $n \in \mathbb{N}$, the graph of f^{2^n} in the corresponding box resembles that in Fig 1-(b). For $\mu > \mu_\infty$, there exists an n such that $f_\mu^{2^n}$

has a horseshoe. That is to say, the hump of $f_\mu^{2^n}$ protrudes through the bottom or the top of the box, or equivalently f is said to be finitely renormalizable. Pictorially, the graph of $f_\mu^{2^n}$ in the corresponding box looks like that of in Fig 1-(c). This completes the process of the period-doubling route to chaos.

4.1 Numerical Simulations

We now turn our attention to a piecewise smooth map. Let's begin with the consideration of the tent map

$$T_\lambda(x) = \begin{cases} \lambda x, & 0 \leq x \leq \frac{1}{2}, \\ \lambda(1-x), & \frac{1}{2} \leq x \leq 1. \end{cases}$$

For $\lambda < 1$, 0 is the globally attracting fixed point. For $\lambda = 1$, the points in the set $[0, \frac{1}{2}]$ are the attracting fixed points. For $\lambda > 1$, one considers the graph of $T_\lambda^2(x)$ in the box.

If the renormalization operator (see e.g., (54)) R on $[\hat{p}_\lambda, p_\lambda]$ is introduced, then

$$(RT_\lambda)(x) = \begin{cases} \lambda^2 x, & 0 \leq x \leq \frac{1}{2}, \\ \lambda^2(1-x), & \frac{1}{2} \leq x \leq 1. \end{cases}$$

Specifically, $RT_\lambda := L_\lambda \circ T_\lambda^2 \circ L_\lambda^{-1}(x)$ is topological conjugate to T_λ on $[\hat{p}_\lambda, p_\lambda]$ through an affine map $L_\lambda(x) = \frac{1}{\hat{p}_\lambda - p_\lambda}(x - p_\lambda)$. Note that RT_λ resembles the graph of the original tent map with a different λ -value. In fact, λ^2 is in place of λ . Since $\lambda > 1$, if the process is to repeat, the "hump" of $T_\lambda^{2^n}$ will eventually protrude through the bottom or the top of the box at finite time. In other words, for $\lambda > 1$, there exists an $n \in \mathbb{N}$ such that $T_\lambda^{2^n}$ possesses a horseshoe or T_λ is finitely renormalizable. Thus, the route to chaos for the tent map through finite period-doubling, or the zero period-doubling to be exact.

These two examples motivate us to consider the following nonsmooth map

$$g_\mu(x) = \begin{cases} \frac{\mu}{2}x =: f_1(x) & 0 \leq x \leq \frac{1}{2} \\ \mu x(1-x) & \frac{1}{2} \leq x \leq 1. \end{cases} \quad (1)$$

The map is the hybrid of the tent map, which is nonconcave, and the quadratic map, which is concave on $(\frac{1}{2}, 1)$. It is expected that a finite period-doubling cascade is to occur. To see this, we compute the bifurcation diagram for the family g_μ , see Fig 2.

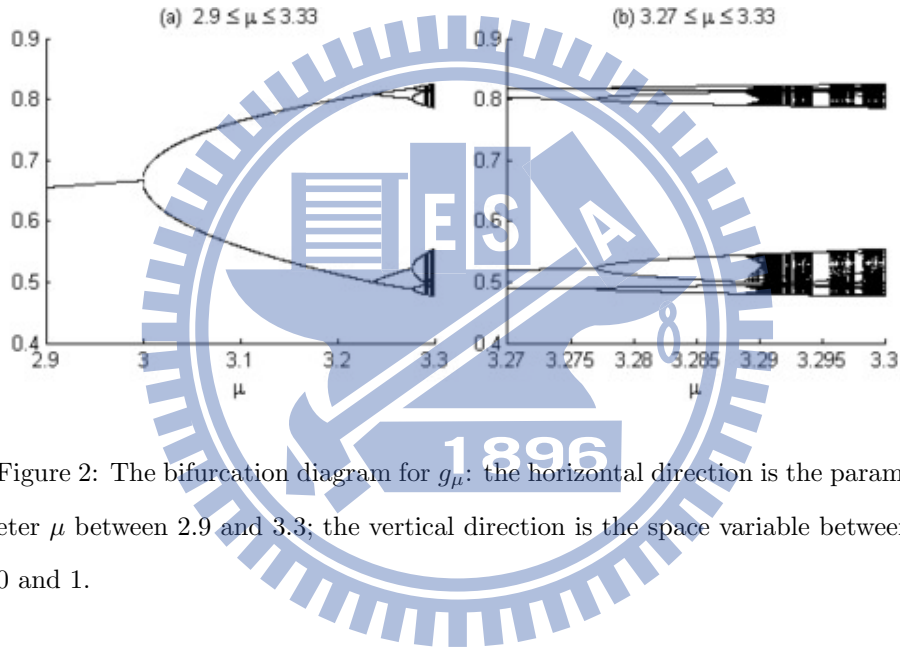


Figure 2: The bifurcation diagram for g_μ : the horizontal direction is the parameter μ between 2.9 and 3.3; the vertical direction is the space variable between 0 and 1.

Indeed, our numerical calculation demonstrates that as one increases μ from one the following scenarios occurs: for $1 < \mu < \mu_1 \approx 3$, g has a stable fixed point. For $\mu_1 < \mu < \mu_2 \approx 3.2361$, a stable period two orbit is born while the fixed point becomes unstable. While the process repeats itself until $\mu = \mu_6 \approx 3.28876826$ in which case the 2^5 period point becomes neutral stable and the period-doubling process abruptly stops. That is, as long as $\mu > \mu_6$, the corresponding map is finitely renormalizable and the map $g_\mu^{2^6}$ has a horseshoe. To further verify this numerically, we consider $g_\mu^{2^5}(x)$ on $[\hat{p}_{\mu,4}, p_{\mu,4}]$, where $\mu_5 \approx 3.288757 < \mu < \mu_6$. Note that for this range of μ , $p_{\mu,5}$ is a stable period 2^5 point and no period

2^6 point exists, see Fig 3. For $\mu = 3.28876826$, we have that the graph of g^{2^5} extends out of the box, see Fig 4. Such finite period-doubling route is summarized in the Table 1.

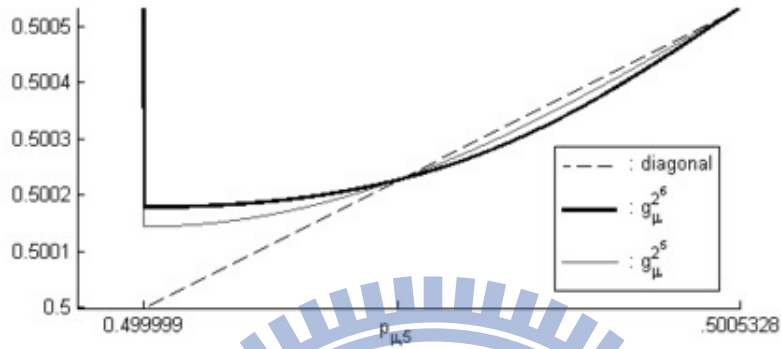


Figure 3: The graphs of $g_\mu^{2^5}$ and $g_\mu^{2^6}$ for $\mu = 3.28876$.

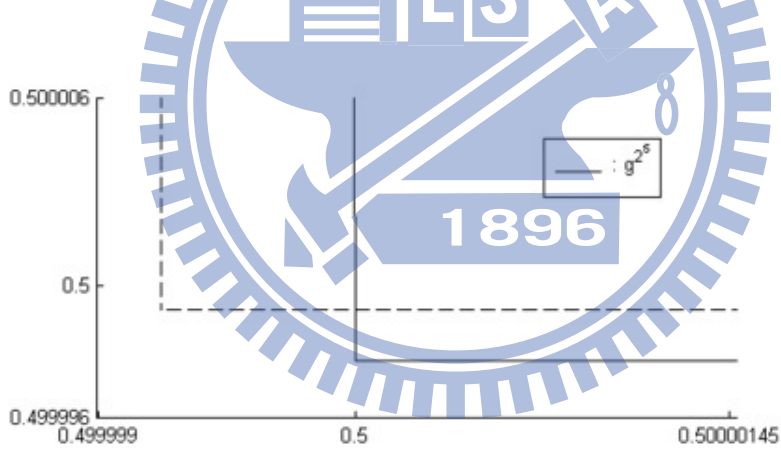


Figure 4: The solid line is a part of the graph of $g_\mu^{2^5}$ for $\mu = 3.28876826$ near the critical point $\frac{1}{2}$, and the dotted lines are a portion of the box $[\hat{p}_{\mu,4}, p_{\mu,4}] \times [\hat{p}_{\mu,4}, p_{\mu,4}]$.

$1 < \mu < \mu_1$ ($\mu_1 \approx 3$)	stable fixed point
$\mu_1 < \mu < \mu_2$ ($\mu_2 \approx 3.2361$)	stable period 2^1 point
$\mu_2 < \mu < \mu_3$ ($\mu_3 \approx 3.2768$)	stable period 2^2 point
$\mu_3 < \mu < \mu_4$ ($\mu_4 \approx 3.28873$)	stable period 2^3 point
$\mu_4 < \mu < \mu_5$ ($\mu_5 \approx 3.288757$)	stable period 2^4 point
$\mu_5 < \mu < \mu_6$ ($\mu_6 \approx 3.28876826$)	stable period 2^5 point
$\mu > \mu_6$	chaotic attractor

Table 1: Bifurcation values for g_μ . As $\mu \geq \mu_6$, the bifurcation abruptly ends and a chaotic attractor occurs.

In fact, we also expect that if $f_1(x)$, given in 4.1 equation(1), is replaced by another convex function on $[0, \frac{1}{2}]$, then the resulting map called h_μ has a finite period doubling cascade to chaos. Intuitively, one sees that the box for h_μ^2 also is smaller than that of g_μ^2 , and that their humps have the same height, see Fig 5. Thus, if g_μ has a finite period-doubling cascade to chaos, then so should have h_μ . To see this numerically, let $h_1(x) = (\mu - 2)x^2 + x$. Define

$$h_\mu(x) = \begin{cases} h_1(x), & 0 \leq x \leq \frac{1}{2}, \\ \mu x(1-x), & \frac{1}{2} \leq x \leq 1. \end{cases} \quad (2)$$

The bifurcation diagram for h_μ , summarized in Table 2, indeed shows the finite period-doubling cascade. It is not surprising to see that as the parameter μ varies, h_μ generates the chaotic attractor quicker than that of g_μ .

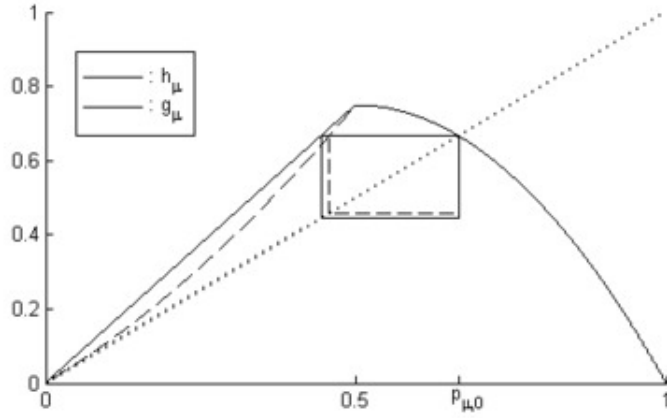


Figure 5: The solid line is the graph of g_μ with $\mu = 3$. Its corresponding box is represented by solid lines. The dotted curve is the graph of the convex function $h_1(x)$. Part of its corresponding box is denoted by dotted lines.

$1 < \mu < \mu_1$ ($\mu_1 \approx 3$)	stable fixed point
$\mu_1 < \mu < \mu_2$ ($\mu_2 \approx 3.2361$)	stable period 2^1 point
$\mu_2 < \mu < \mu_3$ ($\mu_3 \approx 3.2569$)	stable period 2^2 point
$\mu_3 < \mu < \mu_4$ ($\mu_4 \approx 3.26331$)	stable period 2^3 point
$\mu_4 < \mu < \mu_5$ ($\mu_5 \approx 3.263316$)	stable period 2^4 point
$\mu_5 < \mu < \mu_6$ ($\mu_6 \approx 3.26331703824$)	stable period 2^5 point
$\mu > \mu_6$	chaotic attractor

Table 2: Bifurcation values for h_μ . At $\mu > \mu_6$, the bifurcation comes a sudden end and a chaotic attractor appears.

Even though the examples provided here whose nonsmooth points are all at

turning points, such restrictions are not necessary. For instance, if the convex piece of g_μ in equation(1) is defined on $0 \leq x \leq a$ while the concave piece is defined on $a \leq x \leq 1$, where $p_{\mu,0} > a > \hat{p}_{\mu,0}$, then the resulting g_μ also has a finite period-doubling route to chaos.

4.2 Applications

How general is the above route to chaos? To address this question, we now give three more numerical examples.

(i) **Coupling forest trees with limited pollen availability** [1-2]. The dynamics on its synchronous manifold is described by $f_{d,\beta} : [-1 + d, 1] \rightarrow [-1 + d, 1]$ of the form

$$f_{d,\beta}(x) = \begin{cases} x + 1 =: f_1(x), & \text{if } x \leq 0, \\ -dx^{\beta+1} + 1 =: f_{2,d,\beta}(x) & \text{if } x > 0. \end{cases} \quad (3)$$

Here $d > 0$ is a depletion coefficient and $\beta \geq 0$ is the coupling strength. Since $f_{2,d,\beta}(x)$ is concave down for $x > 0$, it behaves like a quadratic map. Like $g_\mu(x)$, $f_{d,\beta}(x)$ consists of two part, one part, which is concave, has a tendency of producing period-doubling cascade to chaos while another part, which is non-concave, produces only simple dynamics. It is expected that $f_{d,\beta}(x)$ should have a finite period-doubling cascade to chaos. This is supported by our numerical computation, see Table 3. In Table 3, β is fixed to be 1, we let d increase from $d_0 \approx 0.75$ to $d_7 \approx 1.1628237$. The corresponding map undertakes a finite period-doubling. As d moves past d_7 , a chaotic attractor occurs. We remark that such finite period-doubling route to chaos holds true for any arbitrary fixed $\beta > 0$.

$0 < d < d_0$ ($d_0 \approx 0.75$)	stable fixed point
$d_0 < d < d_1$ ($d_1 \approx 1.1310$)	stable period 2^1 point
$d_1 < d < d_2$ ($d_2 \approx 1.1620$)	stable period 2^2 point
$d_2 < d < d_3$ ($d_3 \approx 1.1626$)	stable period 2^3 point
$d_3 < d < d_4$ ($d_4 \approx 1.162823313$)	stable period 2^4 point
$d_4 < d < d_5$ ($d_5 \approx 1.162823323$)	stable period 2^5 point
$d_5 < d < d_6$ ($d_6 \approx 1.1628233264$)	stable period 2^6 point
$d_6 < d < d_7$ ($d_7 \approx 1.1628237$)	stable period 2^7 point
$d > d_7$	chaotic attractor

Table 3: Bifurcation values for $f_{d,1}$. At $d > d_7$, the bifurcation comes a sudden end and a chaotic attractor appears.

(ii) **An impact oscillator.** In [27], a method for deriving the global form of the stroboscopic map for the impact oscillator which considers the linear dynamics on either side of the grazing bifurcation was presented. The corresponding regularized discontinuous map has the following form [27]:

$$f(x; \lambda_1, \lambda_2, \mu, \epsilon) = \begin{cases} f_1(x), & \text{if } x < 0, \\ f_2(x), & \text{if } 0 \leq x < \epsilon, \\ f_3(x), & \text{if } x \geq \epsilon. \end{cases} \quad (4)$$

Here $f_1(x) = \lambda_1 x + \mu$, $f_2(x) = -\sqrt{\frac{4x}{\epsilon}} + (\lambda_2 + \frac{1}{\epsilon})x + \mu$ and $f_3(x) = \lambda_2 x + \mu - 1$.

The graphs of f , f^2 and f^4 for $\lambda_1 = 0.7$, $\lambda_2 = -0.9$, $\epsilon = 1$ and $\mu = 1.2$ are shown in Fig 6.

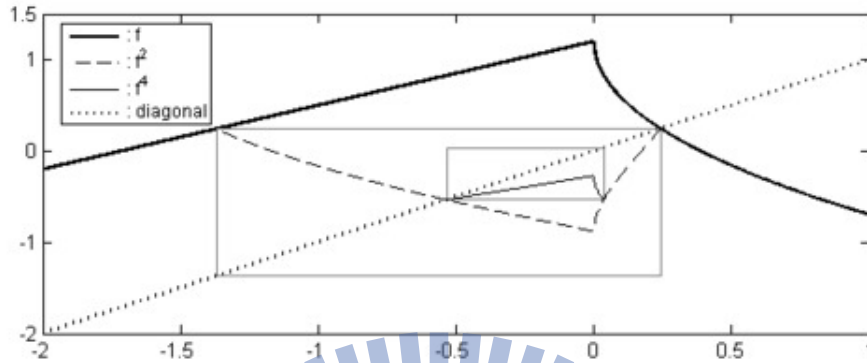


Figure 6: The graphs of f , f^2 and f^4 for $\lambda_1 = 0.7$, $\lambda_2 = -0.9$, $\mu = 1.2$ and $\epsilon = 1$.

One part of the graph $y = f_1(x)$ is a line segment with slope 0.7 which is nonconvex and yields only simple dynamics. The remaining part of the graph, particularly near the turning point $x = 0$, is described by a square root map, which is convex and capable of generating a chaos set without transition. Such map has a stable period two orbit and no chaotic set. As μ decreases, say, to $\mu = 0.795$, the stable period two orbit is still preserved. However, a chaotic set, a cantor set of measure zero, is created, see Fig 7.

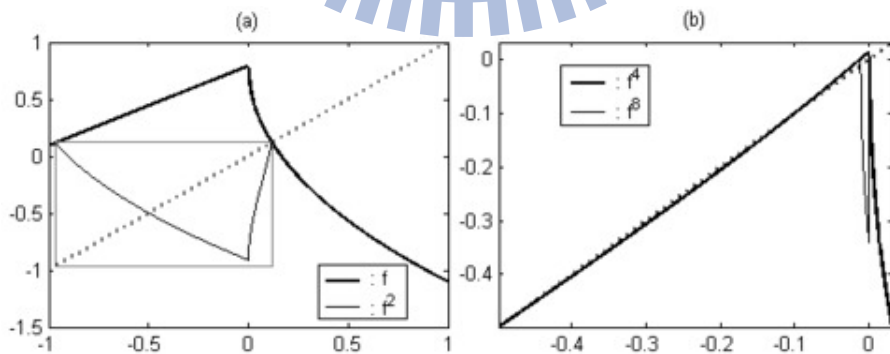


Figure 7: The graphs of (a) f , f^2 and (b) f^4 , f^8 for $\lambda_1 = 0.7$, $\lambda_2 = -0.9$, $\mu = 0.795$ and $\epsilon = 1$.

Note that in Fig 7(b), f^8 extends out of the box. Therefore, an invariant cantor set whose dynamics is conjugate to the shift map of two symbols is generated. In real applications, we are more interested in finding an attractor. As μ keeps decreasing, the stable period two and the chaotic set of measure zero remain coexisted until μ reaches around 0.772891. By then, the period two orbit becomes unstable and f^4 extends out of the box B_2 and still stays in the box B_1 , see Fig 8.

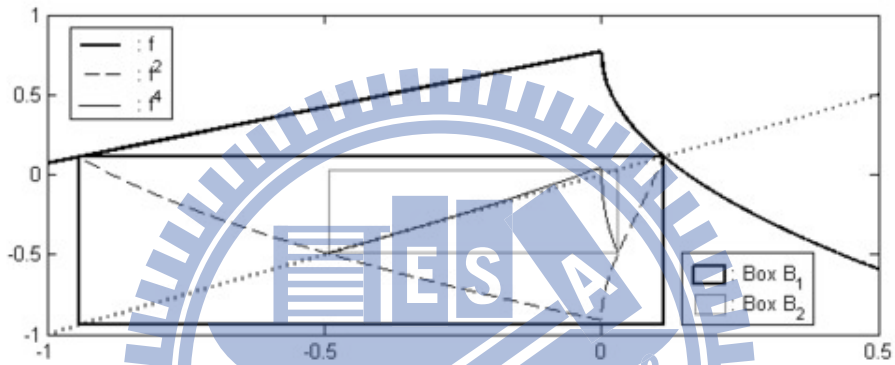


Figure 8: The graphs of f , f^2 and f^4 for $\lambda_1 = 0.7$, $\lambda_2 = -0.9$, $\mu = 0.772$ and $\epsilon = 1$.

Consequently, a chaotic attractor is born. This completes a finite period doubling route to chaos, which is summarized in Table 4.

$0.80523 < \mu < 1.2$	stable period 2
$0.772891 < \mu < 0.805232$	stable period 2 + chaotic set
$0.7 < \mu < 0.772891$	chaotic attractor

Table 4: Bifurcation values for the piecewise linear map $f(\cdot; 0.7, -0.9, \mu, 1)$.

For smaller ϵ , the corresponding f also exhibits a similar route to chaos. The numerical computation of $f(x; 0.7, -0.9, \mu, \lambda)$ as μ varies from 0.2 to 0.155 is summarized in Table 5.

$\mu_0 < \mu < 0.2$ ($\mu_0 \approx 0.1613646$)	stable period 4 point + chaotic set
$\mu_1 < \mu < \mu_0$ ($\mu_1 \approx 0.1580433$)	stable period 8 point + chaotic set
$0.155 < \mu < \mu_1$	chaotic attractor

Table 5: Bifurcation values for $f(\cdot; 0.7, -0.9, \mu, 0.07)$. As μ decreases from 0.2 to 0.155, the bifurcation comes a sudden end and a chaotic attractors appears.

(iii) **Friction oscillator and DC-DC buck converter** (see [44]) Even simpler than square-root maps are those that are completely linear in each of two halves of their domain. Maps of this form can be used to explain the dynamics observed in the friction oscillator and DC-DC converter case studies (see e.g., [44]). Those maps, without loss of generality, can be written in the form

$$f(x) = \begin{cases} f_1(x) = \alpha x + \mu & \text{if } x \leq 0, \\ f_2(x) = \beta x + \mu, & \text{if } x > 0. \end{cases} \quad (5)$$

The most interesting dynamics occurs for $\alpha > 0$ and $\beta < 0$. Indeed, we let $\mu = 1$, $\alpha = 0.4$ and let β vary from -6 to -6.4 . The system undergoes the finite period-doubling. See Table 6 and Fig 9.

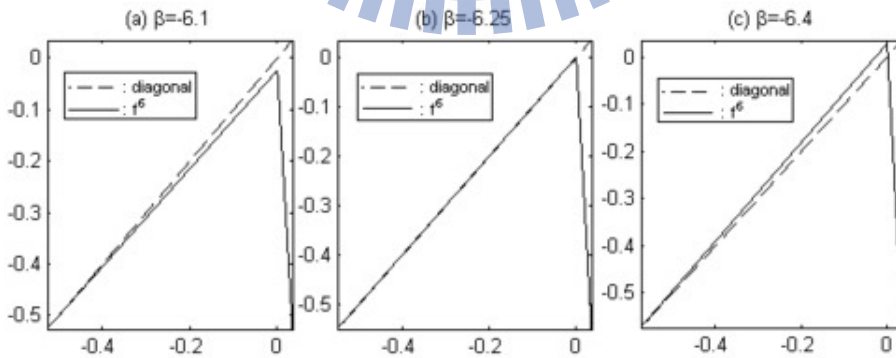


Figure 9: The graph of f^6 for $\beta = -6.1$, $\beta = -6.25$ and $\beta = -6.4$, respectively.

Fig 9(a) is the box where $f^6|_{[-0.5,0]}$ with $\beta = -6.1$ stays. Stable period three point of f is situated at the lower left corner. As β decreases to -6.25 , a portion of the graph of f^6 is coincide with the diagonal. Consequently, a stable period 6 is born. When β decreases past -6.25 , the slope of both pieces of segments of f^6 inside the box have absolute values greater than 1. Hence, like tent map, the chaotic dynamic instantly begins. If one further decreases the value of β , then the period-adding bifurcations also occur.

$-6.25 < \beta < -6$	stable period 3 + chaotic set
$\beta = -6.25$	stable period 6 + chaotic set
$-6.4 < \beta < -6.25$	chaotic attractor

Table 6: Bifurcation values for the piecewise linear map f .

5 Conclusion

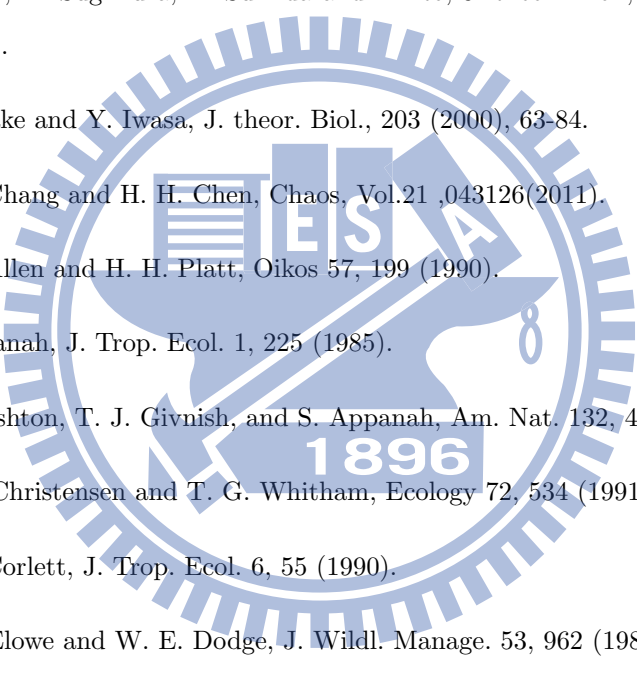
Satake and Iwasa proved that the generalized budget resource model is chaotic when $d > 1$ by computing the Lyapunov exponent. In [3], the model was shown to have Devaney's chaos on an invariant set by proving its topological entropy is positive for $d > 1.00026$. In this thesis, we clearly point out that the generalized resource budget model is chaotic in the sense of Devaney as the depletion coefficient $d > 1$ on an invariant set.

The second part of thesis, we present a *finite period-doubling* route to chaos for a class of nonsmooth maps. Those maps are piecewise smooth functions, which consists of nonconvex and nonconcave parts. Each part may generate a certain type of dynamics as a parameter of the system changes so that when combined together a finite period doubling route to chaos is created. For instance, it could have that one piece of the function, as the system parameter varies, tends to chaos through period-doubling cascades while the other piece produces chaos without transition. The maps defined in (1) and (2) fit into the combination described above. Both maps (4) and (5) has a nonconcave

piece, which is capable of generating chaos without transition, and a nonconvex part yielding only simple dynamics. The third possibility comes from map (3), for which its nonconvex part's route to chaos is through period-doubling. Note that its nonconcave piece produces a simple dynamics. The competition between these two pieces seems to be the mechanism for producing a finite period-doubling route to chaos. No one seems to win out. The numerical computation seems also suggest that the finite period doubling route to chaos for nonsmooth maps is generic.



Bibliography

- 
- [1] Y. Isagi, K. Sugimura, A. Sumida and H. Ito, *J. theor. Biol.*, 187 (1997), 231-249.
- [2] A. Satake and Y. Iwasa, *J. theor. Biol.*, 203 (2000), 63-84.
- [3] S. M. Chang and H. H. Chen, *Chaos*, Vol.21 ,043126(2011).
- [4] R. B. Allen and H. H. Platt, *Oikos* 57, 199 (1990).
- [5] S. Appanah, *J. Trop. Ecol.* 1, 225 (1985).
- [6] P. S. Ashton, T. J. Givnish, and S. Appanah, *Am. Nat.* 132, 44 (1988).
- [7] K. M. Christensen and T. G. Whitham, *Ecology* 72, 534 (1991).
- [8] R. T. Corlett, *J. Trop. Ecol.* 6, 55 (1990).
- [9] K. D. Elowe and W. E. Dodge, *J. Wildl. Manage.* 53, 962 (1989).
- [10] G. A. Felhammer, T. P. Kilbane, and D. W. Sharp, *J. Wildl. Manage.* 53, 292 (1989).
- [11] P. P. Feret, R. E. Dreh, S. A. Merkle, and R. G. Oderwald, *Bot. Gaz.* 143, 216 (1982).
- [12] L. W. Gysel, *J. Wildl. Manage.* 35, 516 (1971).
- [13] R. A. Ims, *Trends Ecol. Evol.* 5, 135 (1990).
- [14] R. A. Ims, *Am. Nat.* 136, 485 (1990).

- [15] D. H. Janzen, *Annu. Rev. Ecol. Syst.* 2, 465 (1971).
- [16] D. H. Janzen, *Annu. Rev. Ecol. Syst.* 7, 347 (1976).
- [17] H. Kawada and K. Maruyama, *Jpn. J. Ecol.* 36, 3 (1986).
- [18] D. Kelly, *Trends Ecol. Evol.* 9, 465 (1994).
- [19] W. D. Koenig, R. L. Mumme, W. J. Carmen, and M. T. Stanback, *Ecology* 75, 99 (1994).
- [20] D. A. Norton and D. Kelly, *Funct. Ecol.* 2, 399 (1988).
- [21] G. E. Rehfeldt, A. R. Stage, and R. T. Bingham, *Forensic Sci.* 17, 454 (1971).
- [22] W. M. Sharp and V. G. Sprague, *Ecology* 48, 243 (1967).
- [23] J. W. Silvertown, *Biol. J. Linn. Soc.* 14, 235 (1980).
- [24] C. C. Smith, J. L. Hamrick, and C. L. Kramer, *Am. Nat.* 136, 154 (1990).
- [25] V. L. Sork, J. Bramble, and O. Sexton, *Ecology* 74, 528(1993).231-249 (1997).
- [26] N. Hinrichs, M. Oestreich and K. Popp, *Journal of Sound Vibration*, 216(3) (1998), 435-459.
- [27] S. R. Pring and C. J. Budd, *SIAM J. Appl. Dyn. Syst.* 9, No. 1 (2010), 188-219.
- [28] S.J. Hogan, L. Higham, and T.C.L. Griffin, *R. Soc. Lond. Proc. Ser. A Math. Phys. Eng. Sci*, 463 (2007), pp. 49V65.
- [29] J.P. Keener, *Trans. Amer. Math. Soc.*, 261 (1980), pp. 589V604.
- [30] M. A. Harrison and Y. -C. Lai, *Phys. Rev. E*, Vol. 59, No. 4 (1999), 3799-3802.
- [31] M. J. Feigenbaum, *J. Stat. Phys.* 19, No. 1 (1978), 25-52.

- [32] Y. Pomeau and P. Manneville, *Commun. Math. Phys.* 74, No. 2 (1980), 189-197.
- [33] C. Grebogi et al., *Phys. Rev. Lett.* 48, No. 22 (1982), 1507-1510.
- [34] D. Ruelle and F. Takens, *Commun. Math. Phys.* 20, No. 3 (1971), 167-192; 23, No. 4 (1971), 343-344.
- [35] S. Newhouse, D. Ruelle and F. Takens, *Commun. Math. Phys.* 64, No. 1 (1978), 35-40.
- [36] B. Brogliato, Springer-Verlag, New-York, 1999.
- [37] B. Brogliato, Springer-Verlag, New York, 2000. *Lecture Notes in Physics*, Volumn 551.
- [38] M. Kunze, Springer-Verlag, Berlin, 2000. *Lecture Notes in Mathematics*, Volumn 1744.
- [39] R. I. Leine and H. Nijmeijer, Springer-Verlag, 2004.
- [40] E. Mosekilde and Zh. Zhusubalyev, World Scientific, 2003.
- [41] M. Wiercigroch and B. de Kraker, World Scientific Publishing, 2000.
- [42] B. Blazejczyk-Okolewska, K. Czolczynski and J. Kapitaniak, T. Wojewoda, World Scientific, Singapore, 1999.
- [43] M. di Barnado, C. J. Budd, A. R. Champneys and P. Nowalczyk, Springer, N. Y. 2004.
- [44] M. di Barnado, C. J. Budd, A. R. Champneys and P. Nowalczyk, Springer-Verlag London Limited, 2008.
- [45] R. L. Devaney, *An Introduction to Chaotic Dynamical Systems*, 2nd ed. (Addison-Wesley, Redwood City, Canada, 1989).
- [46] C. Robinson, *Dynamical Systems: Stability, Symbolic Dynamics, and Chaos*, 2nd ed. (CRC, Boca Raton, FL, 1998).

- [47] M. Misiurewicz, Bull. Acad. Pol. Sci., Ser. Sci. Math., Astron. Phys. 27, 167 (1979)
- [48] D. Kwietniak and M. Misiurewicz, Qual. Theory Dyn. Syst. 6, 169 (2005).
- [49] C. Li and G. Chen, Chaos 14, 343 (2004).
- [50] S. Li, Trans. Am. Math. Soc. 339, 243 (1993).
- [51] Wellington de Melo and Sebastian van Strien, One-Dimensional Dynamics, 1nd ed.
- [52] W. de Melo and S. van Strien, Springer-Verlag Berlen Heidelberg, 1993.
- [53] A. Katok and B. Hasselblatt, Cambridge University Press, 1995.
- [54] Robert L. Devaney, Addison-Wesley Publishing Company, Inc., 1994.

